Available online at www.sciencedirect.com
ScienceDirect
Polymer 48 (2007) 4005–4014
polymer
www.elsevier.com/locate/polymer

An in situ matrix functionalization approach to structure stability enhancement in polyethylene/montmorillonite nanocomposites prepared by intercalative polymerization

Yingjuan Huang, Kefang Yang[1], Jin-Yong Dong*

CAS Key Laboratory of Engineering Plastics, Joint Laboratory of Polymer Science and Materials, Institute of Chemistry, Chinese Academy of Sciences, Beijing 100080, China

Received 20 March 2007; received in revised form 14 May 2007; accepted 16 May 2007
Available online 21 May 2007

Abstract

This paper discusses a strategy of enhancing the structure stability of polyethylene/montmorillonite (PE/MMT) nanocomposites prepared by intercalative polymerization technique. The chemistry centers on an in situ, controlled PE matrix functionalization that is made possible by engaging a reactive comonomer in the intercalative polymerization process to intentionally anchor in the formed PE matrix ready-to-functionalize reactive groups. Thus, ethylene polymerization was conducted in the presence of *p*-methylstyrene (*p*-MS) using an OMMT (organically modified MMT)-intercalated metallocene catalyst ($Et[Ind]_2ZrCl_2$ in combination with MAO), resulting in *p*-MS-containing PE/OMMT nanocomposites. Subsequent functionalization of the PE matrix then facilely and selectively occurred on the benzyl group in the *p*-MS unit, including a free radical maleation reaction and a butyllithium-initiated metallation reaction which was followed by an anionic graft-from polymerization of methyl methacrylate (MMA), under very mild reaction conditions. The in situ-incorporated functional groups, including the pendant maleic anhydride groups and the polar poly(methyl methacrylate) (PMMA) side chains, significantly improved miscibility between the PE matrix and laminated silicate layers of MMT, leading to effective stabilization of the nanocomposite structure against processing.

Keywords: Polyethylene/montmorillonite nanocomposite; Matrix functionalization; Structure stability

1. Introduction

Since the invention of nylon/montmorillonite (MMT) nanocomposites by Toyota researchers in the 1990s [1], the study of MMT-reinforced polymer nanocomposites has been one of the most interesting subjects in both polymer and material research fields [2]. This is because the introduction of a few weight percent of nanometer-scale laminated silicate layers into a polymer matrix can drastically improve many of the polymer properties, such as modulus, strength, heat resistance, anti-flammability and anti-gas permeability, which are usually very difficult to assess by traditional micrometer-scale inorganic fillers [3].

Polyolefins are among the most interesting polymers deemed to benefit the most from the formation of nanocomposite with MMT because of their widespread applications [4]. However, polyolefins are chemically non-polar, which govern its nearly complete immiscibility with MMT and pose great challenges for the preparation of polyolefin/MMT nanocomposites by direct polymer intercalation (including melt and solution intercalations) [5]. In order to successfully disperse MMT into nanometer-scale silicate layers in polyolefins to form nanocomposites, one effective approach has been the in situ intercalative polymerization [6], which is conducted by the intercalation of transition metal olefin polymerization catalysts (including Ziegler–Natta, metallocene, and post-metallocene) in the interlayer of an organically modified

* Corresponding author.
E-mail address: jydong@iccas.ac.cn (J.-Y. Dong).
[1] Ph.D. candidate of the Graduate School, Chinese Academy of Sciences, China.

0032-3861/$ - see front matter © 2007 Elsevier Ltd. All rights reserved.
doi:10.1016/j.polymer.2007.05.037

MMT (OMMT) followed by an in situ olefin polymerization. This approach has the advantage of bypassing the thermodynamic obstacles associated with direct polymer intercalation, and leads to satisfactory MMT nanometer-scale dispersions in polyolefins. In fact, the in situ intercalative polymerization technique has been generally applied to prepare polyolefin/MMT nanocomposites [7–10]. There are abundant evidences available to show it is more desirable in terms of effectiveness to form nanocomposite structure than a melt or solution polymer intercalation assisted by functional polyolefin compatilizers [11–14,30].

However, despite the claimed successes of the in situ intercalative polymerization methodology, theoretical studies show such a dispersion of MMT in polyolefins (the nanocomposite structure) is thermodynamically unstable [15,16]. This is actually conceivable because of the inherent immiscibility between the non-polar polyolefins and the polar inorganic MMT. Experimentally, it is also observed that after high-temperature processing the nanocomposite structure (the dispersion of the nanometer-scale silicate layers of MMT) of the polyolefin/MMT hybrids formed by intercalative polymerization more or less (depending on the processing conditions) collapse and low *d*-spacing parallel stacks of silicate layers are recovered to form a conventional micrometer-scale filling structure [10,17].

As a part of our research, we have been exploring ways to improve the structure stability of polyolefin/MMT nanocomposites prepared by intercalative polymerization, trying to make the promising technology more reliable for a future practical application [18]. Recently, we proposed a simultaneous polyolefin matrix functionalization approach that experimentally proved quite effective in gaining that goal [19]. In this approach, a polar vinyl monomer 10-undecen-1-ol was engaged in the intercalative polymerization of ethylene using an OMMT-intercalated metallocene catalyst to prepare polyethylene (PE)/MMT nanocomposites. The copolymerization between ethylene and 10-undecen-1-ol gave rise to functionalized PE matrix bearing hydroxyl (–OH) groups. These simultaneously incorporated –OH groups in the PE matrix induced strong interactions between the polymer matrix and the laminated silicate layers of MMT (due to hydrogen bonding), prompting effective stabilization of the nanocomposite structure right during its formation. However, one major drawback of this approach is the requirement of direct functional copolymerization with a polar monomer, which is known to be inconvenient for Ziegler–Natta and metallocene polymerizations because of the unavoidability of catalyst poisoning by heteroatom (i.e. O, N, etc.)-containing polar groups [20]. In fact, only few functional monomers with specifically designed steric and electronic structures, represented by 10-undecen-1-ol, have been reported to be able to accomplish successful copolymerization with ethylene or propylene using Ziegler–Natta and metallocene or even the less oxophilic late transition metal catalysts [21–23]. The direct functional copolymerization with polar vinyl monomers has yet to be mature as a practical route to polyolefin functionalization.

Trying to avoid direct engagement of a polar monomer in polymerization, we recently developed an alternative way to reach the goal of polyolefin matrix functionalization in the preparation of polyolefin/MMT nanocomposites by intercalative polymerization. In this method, a selected reactive comonomer (i.e. *p*-methylstyrene, *p*-MS) free of any catalyst-poisoning heteroatoms was involved in the intercalative polymerization. The resultant nanocomposite was therefore based on a reactive polyolefin matrix bearing ready-to-functionalize reactive groups. This reactive polyolefin matrix underwent facile and controlled functionalization reactions under mild reaction conditions to leave the polymerization-formed nanocomposite structure intact. The in situ-incorporated functional groups, including maleic anhydride (MA) and methyl methacrylate monomer unit (MMA), were able to boost the interfacial interaction between the polyolefin matrix and the laminated silicate layers of MMT, leading to effective stabilization of the nanocomposite structure against processing.

2. Experimental section

2.1. Materials and instrumentation

All O_2- and moisture-sensitive manipulations were carried out inside an argon filled Vacuum Atmosphere dry-box equipped with a dry train. CP grade toluene, benzene, and THF were deoxygenated by argon purge before refluxing for 48 h and distilling over sodium. MAO (1.4 M in toluene) was purchased from Albermarle and used as received. *rac*-Et[Ind]$_2$ZrCl$_2$, maleic anhydride (MA), benzoyl peroxide (BPO), *n*-BuLi (2.79 M in hexane), and *N*,*N*,*N*′,*N*′-tetramethylethylene diamine (TMEDA) were purchased from Aldrich. *p*-Methylstyrene (*p*-MS) and methyl methacrylate (MMA) were from Acros and purified by drying over CaH_2 followed by distillation under reduced pressure. Polymerization grade ethylene was supplied by Yanshan Petrochemical Co. of China. The organically modified MMT (OMMT) containing hexadecyl trimethylammonium surfactant was kindly provided by Professor Zongneng Qi in the same institute, which was prepared from Na^+-MMT (Qinghe Chemical Plant, China) with a cation exchange capacity (CEC) of 100 meq/100 g. The organic content of the OMMT is 30.1 wt%.

All high-temperature ^{1}H NMR spectra were recorded on a Bruker AM-300 instrument in *o*-dichlorobenzene-d_4 at 115 °C. The melting temperatures of the polymers were measured by differential scanning calorimetry (DSC) using a Perkin–Elmer DSC-7 instrument controller at a heating rate of 10 °C min^{-1}. Wide-angle X-ray diffraction (XRD) measurement was performed on a D8 advance X-ray powder diffractometer (Bruker Co.) with Cu Kα radiation ($\lambda =$ 0.15406 nm) at a generator voltage of 40 kV and generator current of 40 mA. The scanned 2θ range was between 1.5° and 40°, at a scanning rate of 2° min^{-1}. The interlayer spacing (d_{001}) of MMT was calculated in accordance with the Bragg equation: $2d\sin\theta = \lambda$. Thermogravimetric analysis (TGA) was performed using a Perkin–Elmer TGA instrument under nitrogen atmosphere with a heating range of 50–700 °C at a heating rate of 20 °C min^{-1}. IR was detected by a Perkin–Elmer FTIR spectrometer using a polymer thin film (about

2–8 μm), which was prepared by compression-molding polymer powders between PTFE coated aluminum sheets at 190 °C and 8.0 kg cm^{-3}. The MA content was calculated from FTIR by the following equation: MA wt% = $K(A_{1780}/d)$, where A_{1780} is the absorbance of carbonyl group at 1780 cm^{-1} and d is the thickness (mm) of the film, K is constant (0.25) and determined by calibration of the known MA content of MA grafted PP. The intrinsic viscosity of polymer was measured in decalin dilute solution at 135 °C with a Cannon-Ubbelohde viscometer. The viscosity-average molecular weight was calculated by the Mark–Houwink equation: $[\eta] = KM^{\alpha}$, where $K = 6.2 \times 10^{-4}$ dL/g and $\alpha = 0.70$. Transmission electron microscopy (TEM) was carried out on a Jeol JEM2011 transmission electron microscope using an acceleration voltage of 200 kV. Samples for TEM were prepared by molding into specimens at 200 °C and microtomed into ultra-thin sections.

2.2. Preparation of OMMT-intercalated metallocene catalyst (OMMT/Et[Ind]$_2$ZrCl$_2$)

To a 500 mL three-necked flask containing 100 mL of toluene was added 5.0 g of OMMT at 60 °C. The suspension was stirred for 2.0 h before 40.0 mL of MAO was introduced into the flask. After stirring for 5.0 h, the content of the flask was filtered to remove excess MAO. The flask was refilled with toluene, after which 0.502 mmol of *rac*-Et[Ind]$_2$ZrCl$_2$ in toluene solution was syringed into the flask. The reaction was allowed to proceed for 10 h. After the reaction was completed, the reactants were subjected to filtration, repeated washing with toluene (5 × 50 mL), and drying under vacuum at 60 °C, to give the OMMT-intercalated Et[Ind]$_2$ZrCl$_2$ catalyst (OMMT/Et[Ind]$_2$ZrCl$_2$) as a gray powder.

2.3. Intercalative copolymerization of ethylene and p-MS using OMMT/Et[Ind]$_2$ZrCl$_2$ and MAO: preparation of PE-co-p-MS/OMMT nanocomposites

The polymerization reactions were carried out with a Parr stainless steel autoclave reactor equipped with a mechanical stirrer. In a typical reaction (run 5 in Table 1), 7.0 mL of *p*-MS (52.5 mmol) was combined with 50.0 mL of toluene and introduced into the reactor. The reactor was then filled with ethylene under a constant pressure of 0.5 MPa. After the reactor had been heated to 50 °C, the powdery OMMT/Et[Ind]$_2$ZrCl$_2$ catalyst (0.156 g, [Zr] = 4.78×10^{-6} mol) was added into the vigorously stirred liquid mixture saturated with ethylene. The polymerization reaction was initiated by charging 2.0 mL of MAO (2.8 mmol) into the reactor using a syringe. After 60 min, the polymerization was quenched by 20 mL of acidified ethanol (containing 10% of HCl). The polymer product was collected by filtration and repeatedly washed with ethanol and acetone. After drying under vacuum at 60 °C for 24 h, 10.39 g of polymer product was obtained in white powder (PE-*co*-*p*-MS/OMMT).

2.4. Maleation of PE-co-p-MS/OMMT and synthesis of (PE-co-p-MS)-g-MA/OMMT nanocomposites

In a typical reaction (run 3 in Table 2), 2.0 g of PE-*co*-*p*-MS/OMMT nanocomposite containing 0.90 mol% of *p*-MS and 1.50 wt% of OMMT (run 5 in Table 1) was suspended in 50 mL of benzene in nitrogen atmosphere. Then 0.80 g of sublimed MAH and 0.40 g of recrystallized BPO were added into the flask. Temperature was brought up to 75 °C by an oil bath. After stirring for 3 h, the content of the flask was poured into 30 mL of acetone. The polymer was isolated by

Table 1
Conditions[a] and results of copolymerization of ethylene and *p*-MS using OMMT/Et[Ind]$_2$ZrCl$_2$–MAO

Run	OMMT/Et[Ind]$_2$ZrCl$_2$ (g)	*p*-MS (mol/L)	Yield (g)	Catalyst activity[b]	*p*-MS in polymer (mol%)	OMMT content (wt%)	T_m (°C)	ΔH (J/g)	M_η ($\times 10^{-4}$ g/mol)
1	0.152	0	1.82	0.39	–	8.35	132.8	153.3	11.7
2	0.143	0.075	2.95	0.67	0.078	4.85	128.8	145.6	10.32
3	0.155	0.15	6.81	1.43	0.094	2.28	127.2	145.0	9.72
4	0.161	0.45	7.64	1.54	0.37	2.11	124.5	141.2	8.20
5	0.156	1.05	10.39	2.17	0.90	1.50	120.2	101.9	5.05

[a] Other conditions: 0.5 MPa ethylene, 50 mL toluene, [MAO]/[Zr] = 600, polymerization temperature = 50 °C, polymerization time = 60 min.
[b] Catalyst activity: $\times 10^{-6}$ g polymer/mol Zr h.

Table 2
A summary of in situ matrix functionalization with MA and PMMA of PE-*co*-*p*-MS/OMMT nanocomposites

Run	Starting PE-*co*-*p*-MS/OMMT (g)	Other reactants and feedings	MA content in polymer (wt%)	PMMA content in polymer (wt%)	M_η after functionalization ($\times 10^{-4}$ g/mol)	M_η before functionalization ($\times 10^{-4}$ g/mol)	T_m (°C)
1[a]	Entry 3 in Table 1/2.0	MA = 0.8 g, BPO = 0.24 g	0.27	–	8.22	9.72	128.0
2[a]	Entry 4 in Table 1/2.0	MA = 0.8 g, BPO = 0.26 g	0.30	–	8.40	8.20	125.4
3[a]	Entry 5 in Table 1/2.0	MA = 0.8 g, BPO = 0.40 g	0.55	–	5.35	5.05	121.5
4[b]	Entry 5 in Table 1/0.8	*n*-BuLi = 8.40 mmol, MMA = 4.65 g	–	10.0	–	5.05	121.2

[a] Other conditions for MA modification: 50 mL benzene, 75 °C, 3 h.
[b] Other conditions for PMMA-grafting modification: for metallation, 50 mL THF, 45 °C, 6 h; for anionic polymerization, 50 mL cyclohexane, 25 °C, 6 h.

filtration and repeatedly washed with acetone until a complete decoloration was accomplished with the polymer. The product was dried under vacuum at 60 °C for 24 h.

2.5. Lithiation of PE-co-p-MS/OMMT and synthesis of (PE-co-p-MS)-g-PMMA/OMMT nanocomposite

PE-*co*-*p*-MS/OMMT (0.8 g) containing 0.90 mol% of *p*-MS and 1.50 wt% of OMMT (run 5 in Table 1) was suspended in 50 mL of anhydrous THF. Metallation reaction was initiated by adding 3.0 mL of *n*-BuLi (2.79 M in hexane) and 0.3 mL of TMEDA into the suspension. The reaction mixture was stirred at 45 °C for 6 h before filtration. The residue was repeatedly washed with hexane. After that, the flask was refilled with 50 mL of cyclohexane, to which was added 5.0 mL of MMA at ambient temperature. The reaction was allowed to proceed for 6 h before termination by methanol. The resulting polymer was filtered, repeatedly washed with THF and acetone, and dried under vacuum at 60 °C for 24 h.

2.6. Compression molding

The compression molding of the nanocomposites was performed using a compression-molding instrument operated at 200 °C under a pressure of 8.0 kg cm^{-3}. The samples were held in the mold at the temperature for 5 min before being cooled to ambient temperature.

3. Results and discussion

p-Methylstyrene (*p*-MS) has been extensively studied by Chung and co-workers as an excellent choice of reactive comonomer under Ziegler–Natta or metallocene catalysis to accomplish controlled polyolefin functionalization [24–28]. Bearing no catalyst-poisoning polar functional groups, *p*-MS performed excellently in copolymerization with ethylene over a bunch of bridged metallocene catalysts having superior copolymerization capabilities. With no significant catalyst activity reduction accompanying, the incorporation of *p*-MS was highly controllable, high *p*-MS incorporations being accessible at high *p*-MS feedings. The intermolecular distribution of *p*-MS in the obtained copolymers was deemed narrow because of the single active site feature of metallocene catalyst, while its intramolecular distribution was generally confirmed random. *p*-MS-incorporated PE as well as other polyolefins were endowed with versatile chemical reactivities toward functionalization. The benzylic protons (ϕ-CH_3) of the incorporated *p*-MS unit were able to undergo, under mild reaction conditions, both free radical maleation reaction and butyllithium-induced metallation reaction, with the latter usually being followed by an anionic graft-from polymerization of methyl methacrylate (MMA), to prepare maleic anhydride-functionalized polyolefins and graft-structured functional polyolefins containing PMMA side chains of controllable length, respectively. On the basis of those meritable background knowledge, in the current research, we employed *p*-MS as a reactive comonomer in the intercalative polymerization of ethylene using an OMMT (organically modified MMT)-intercalated metallocene catalyst (Et[Ind]$_2$ZrCl$_2$ in combination with MAO) to prepare *p*-MS-containing PE/OMMT nanocomposites (PE-*co*-*p*-MS/OMMT). We conceived that the *p*-MS unit incorporated in the PE matrix could render an in situ, controlled PE matrix functionalization under mild reaction conditions to, without inflicting any detriment to the polymerization-formed nanocomposite structure, enhance its stability by promoting miscibility between the polyolefin matrix and exfoliated silicate layers of MMT. In Scheme 1 is illustrated the overall plot.

3.1. Preparation of PE-co-p-MS/OMMT nanocomposites

The OMMT-intercalated metallocene catalyst was prepared by adopting a previously described procedure [19]. OMMT powder was first suspended in toluene to form a homogeneous slurry, then successive treatments with MAO and Et[Ind]$_2$ZrCl$_2$ took place in the same reactor at an elevated temperature. The obtained supported catalyst OMMT/Et[Ind]$_2$ZrCl$_2$ was subjected to Zr and Al content measurements, obtaining values of 0.11 wt% and 12.60 wt% (OMMT contained 1.80 wt% of measurable Al), respectively. OMMT, with a starting interlayer spacing of 2.0 nm, a size similar to that of MAO [29], must have gradually accepted MAO for intercalation and simultaneously expanded the interlayer space to accommodate the metallocene compound. The comparison of XRD patterns of OMMT and OMMT/Et[Ind]$_2$ZrCl$_2$ confirmed the hypothesis, which revealed a distinct shift of (001) diffraction peak for the supported catalyst ($2\theta = 2.28°$, with a secondary and a tertiary peaks at 4.68° and 6.62°) relative to OMMT (4.44°). Correspondingly, *d*-spacing of OMMT/Et[Ind]$_2$ZrCl$_2$ reaches 3.8 nm, ca. 1.8 nm larger than that of OMMT. This size is sufficient for MAO to activate the intercalated metallocene catalyst for the subsequent intercalative polymerization.

Copolymerization of ethylene and *p*-MS using OMMT/Et[Ind]$_2$ZrCl$_2$ and MAO was carried out in toluene solution at 50 °C. Table 1 summarizes the overall conditions and results. In general, the intercalative polymerization of ethylene was not worsened by the presence of *p*-MS. On the contrary, the polymerization reaction was accelerated by *p*-MS, both polymerization yield and catalyst activity per mole of transition metal catalyst increasing with increase of *p*-MS feeding in polymerization, a phenomenon that had been observed in the case of homogeneous ethylene/*p*-MS copolymerization [24,26] where it was reasoned by a kind of "comonomer effect". Both the melting temperature (T_m) and thermal enthalpy (ΔH) of the polymerization products measured by DSC decreased with *p*-MS, a sign of *p*-MS incorporation in PE. To precisely quantify *p*-MS incorporations, the polymerization products were dissolved in $C_2D_2Cl_4$ for ^{1}H NMR analysis.

Fig. 1 compares ^{1}H NMR spectra of three PE-*co*-*p*-MS/OMMT samples containing 0.094, 0.37, and 0.90 mol% of *p*-MS (runs 3, 4, and 5 in Table 1), respectively. In addition to the major chemical shift at $\delta = 1.5$ ppm corresponding to C**H**$_2$ group in PE backbone, all these spectra display three

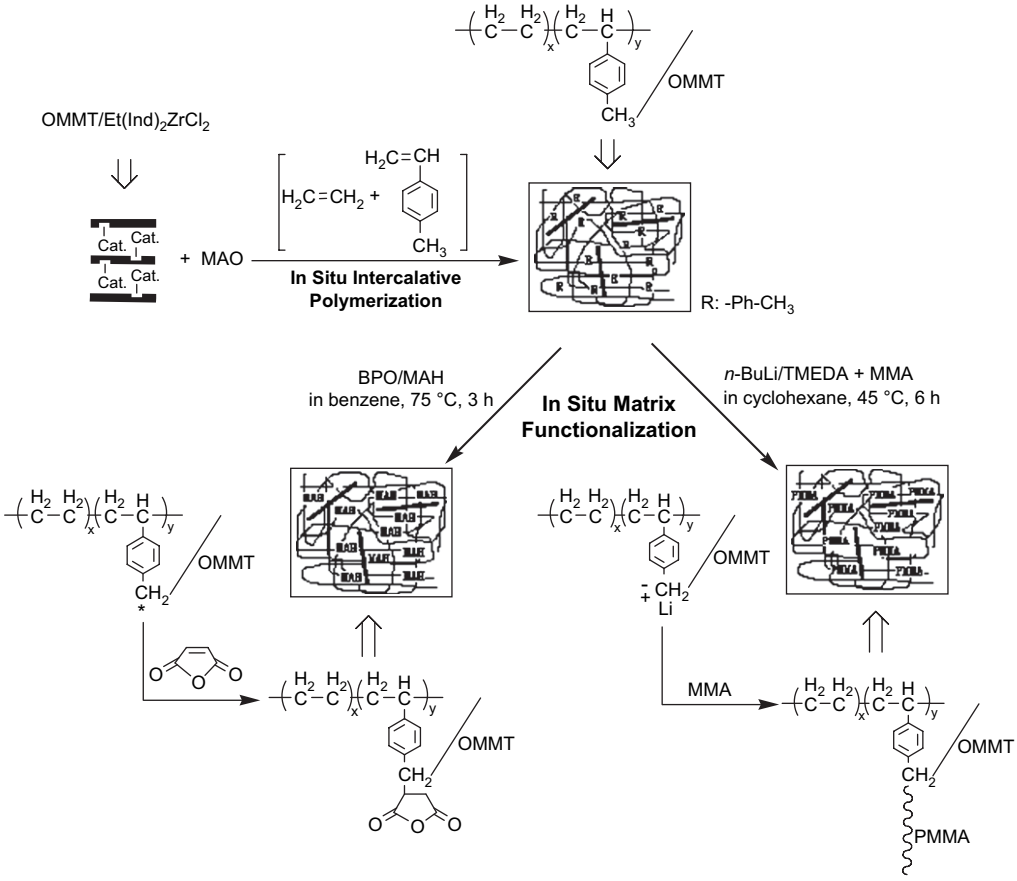

Scheme 1. Preparation of PE-*co*-*p*-MS/OMMT nanocomposite and subsequent in situ matrix functionalization.

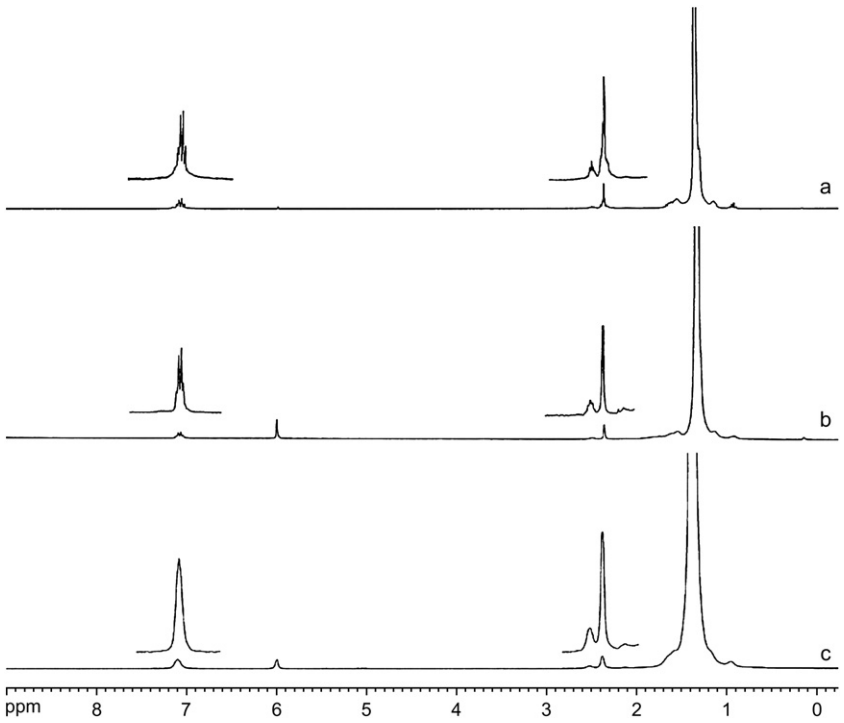

Fig. 1. ^{1}H NMR spectra of three PE-*co*-*p*-MS/OMMT nanocomposites containing (a) 0.094 mol%, (b) 0.37 mol%, and (c) 0.90 mol% of *p*-MS units in the matrix (runs 3, 4, and 5 in Table 1), respectively.

minor chemical shifts at $\delta = 2.35$, 2.50, and 7.10 ppm, corresponding, respectively, to ϕ-C**H**$_3$, $-CH_2-$C**H**(ϕ)$-$, and four aromatic protons in the incorporated *p*-MS unit. To derive the molar percentage of *p*-MS in each sample, the integration of the peak at $\delta = 7.10$ ppm was compared with that of the C**H**$_2$ peak at $\delta = 1.5$ ppm, together with a consideration of number of protons either peak represented. The results are included in Table 1. By contrasting to the original feedings, it is clear that the *p*-MS incorporation in the intercalative copolymerization still follows a general rule of metallocene-catalyzed random copolymerization, i.e., comonomer incorporation exhibits a good dependence on its feeding. In fact, it is very interesting to compare the incorporation vs feeding profiles between ethylene/*p*-MS copolymerization catalyzed by the confined OMMT/Et[Ind]$_2$ZrCl$_2$–MAO catalyst system and that by unconfined, homogeneous Et[Ind]$_2$ZrCl$_2$–MAO system. As demonstrated in Fig. 2, under similar reaction conditions (same polymerization temperature and ethylene pressure, similar catalyst and cocatalyst amounts), the incorporations of *p*-MS with the OMMT/Et[Ind]$_2$ZrCl$_2$ catalyst exhibit a significant inferiority to those with the homogeneous one. This might be explained by a greater extent of hindrance toward *p*-MS, a sterically bulky molecule, than ethylene when they both needed to diffuse into the OMMT-confined space for copolymerization. This result in this sense reassures the intercalative nature of the copolymerization.

Fig. 3 compares DSC curves of three PE-*co*-*p*-MS/OMMT samples (runs 3, 4, and 5 in Table 1) with that of a net PE-based one obtained in the control reaction of ethylene homopolymerization (run 1 in Table 1). Despite the fact that the four samples are of different MMT loadings, the T_m and ΔH data collected therein and the profile pattern of the curves still shed light on the distribution homogeneity of *p*-MS in the PE matrix. Firstly, the sharp decreases of T_m and ΔH from 132.8 °C and 153.3 J/g (for PE homopolymer) to 120.2 °C and 101.9 J/g at a *p*-MS incorporation of only 0.90 mol%

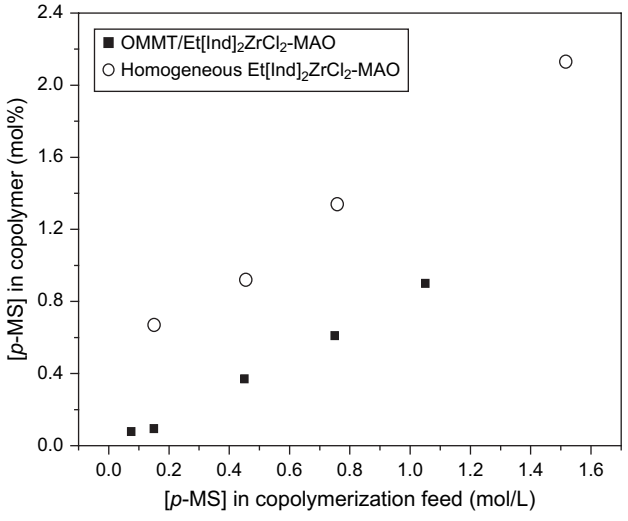

Fig. 2. Comparison of plots of *p*-MS incorporation in PE-*co*-*p*-MS copolymer vs *p*-MS concentration in copolymerization between OMMT/Et[Ind]$_2$ZrCl$_2$–MAO and homogeneous Et[Ind]$_2$ZrCl$_2$–MAO catalyst systems.

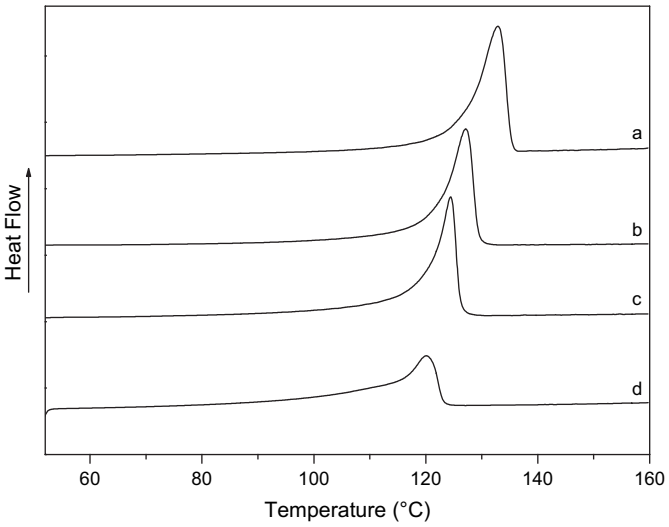

Fig. 3. DSC curves of (a) a net PE/OMMT nanocomposites (run 1 in Table 1) and three PE-*co*-*p*-MS/OMMT nanocomposite samples containing (b) 0.094 mol%, (c) 0.37 mol%, and (d) 0.90 mol% of *p*-MS units in the matrix (runs 3, 4, and 5 in Table 1), respectively.

(run 5 in Table 1) have already revealed largely a good dispersion of *p*-MS units in PE at least at intramolecular level. Secondly, the consistent narrow shapes of the DSC profiles of the copolymer samples could only result from a good intermolecular dispersion of the comonomer.

In order to estimate the average polymer molecular weight, a non-thorough solvent extraction using xylene at 140 °C was conducted on the obtained nanocomposites. The retrieved MMT-free polymer samples were subjected to viscometry to determine their viscosity-average molecular weights (M_η). The results are included in Table 1. With the increase of molar content of *p*-MS, the copolymers show a slight decrease of molecular weight. For all four PE-*co*-*p*-MS/OMMT nanocomposites, the viscosity-average molecular weights of the PE-*co*-*p*-MS copolymers lied in between 9.72×10^4 and 5.05×10^4 g/mol.

Finally, the PE-*co*-*p*-MS/OMMT nanocomposites were subjected to XRD examination to determine both the dispersion state of OMMT in the as-polymerized sample and, if nanocomposite structure had been formed, its stability against processing. First, without heating, the as-polymerized powdery hybrids were amassed in a small stainless steel rectangular chamber (15.0 mm × 15.0 mm × 1.0 mm in size) and compressed into a compact plate using a compression-molding instrument operated at ambient temperature under a pressure of 8.0 kg cm^{-3}. This operation was to dispel the many voids contained in the very loose polymer powder that might interfere with the XRD measurement. Fig. 4A presents XRD patterns of four PE-*co*-*p*-MS/OMMT as-polymerized samples undergoing such a treatment (runs 3, 4, and 5 in Table 1). In fact, despite the different OMMT loadings, all the nanocomposites examined exhibit no discernible (001) diffraction peak of MMT in their respective XRD patterns. This result clearly indicates that exfoliation of OMMT had been achieved in the as-polymerized PE-*co*-*p*-MS/OMMT samples. In other words, we surely obtained PE-*co*-*p*-MS/OMMT nanocomposites that

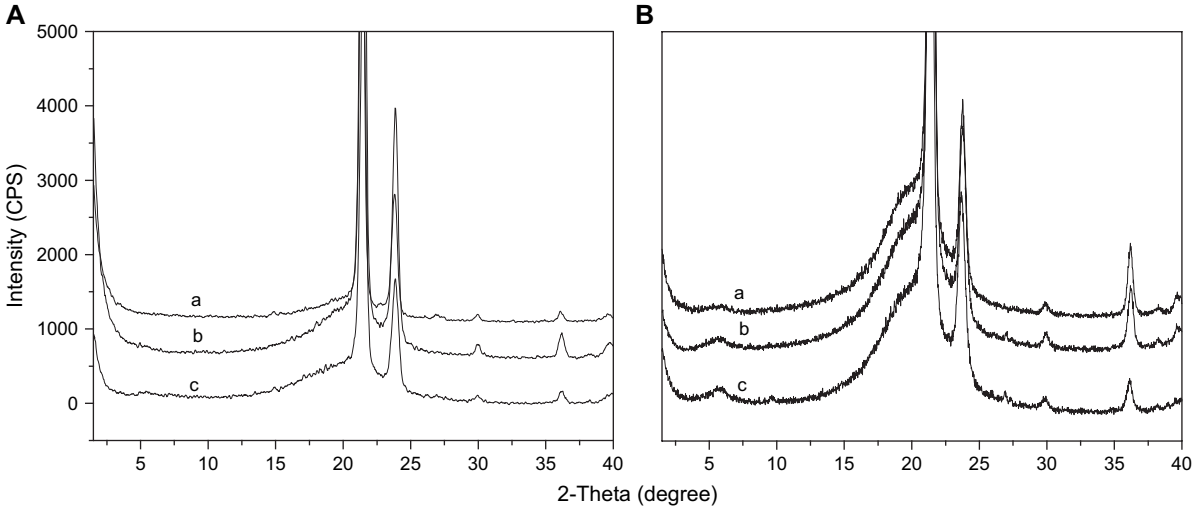

Fig. 4. XRD patterns of (A) as-polymerized and (B) compression-molded PE-*co*-*p*-MS/OMMT nanocomposite samples containing (a) 0.094 mol%, (b) 0.37 mol%, and (c) 0.90 mol% of *p*-MS units in the matrix (runs 3, 4, and 5 in Table 1), respectively.

were based on a *p*-MS-containing PE matrix. Further, the same specimens with confirmed nanocomposite structures were put back into the stainless steel chamber and subjected to melting at 200 °C for 5 min. The thus-treated specimens were reexamined by XRD. The results are shown in Fig. 4B. Without exception, the (001) diffraction peak of MMT reappears in all three measurements, at $2\theta = 5.99-6.23^\circ$ (corresponding to a *d*-spacing of 1.47–1.42 nm). Their results are not surprising, as *p*-MS units incorporated in the PE matrix were still too weak in terms of polarity to promote miscibility with exfoliated silicate layers of OMMT. In consequence, partial, if not all, polymer/inorganic nanocomposite structures collapsed and low *d*-spacing parallel stacks of silicate layers were recovered. Interestingly, it is found that the *d*-spacing values calculated from the newborn peaks in XRD pattern are generally smaller than that of the starting OMMT. This might be due to either decomposition of alkylammonium surfactant in OMMT during heating or a more compact rearrangement of surfactant molecules at elevated temperature. If surfactant decomposition did take place, it would even worsen the immiscible situation of PE and MMT and add to the instability of the nanocomposite structure.

Summarizing the intercalative copolymerization of ethylene with *p*-MS to prepare PE-*co*-*p*-MS/OMMT nanocomposites, *p*-MS functioned effectively as a comonomer using the OMMT-intercalated metallocene catalyst ($Et[Ind]_2ZrCl_2$ and MAO). Reactive PE-*co*-*p*-MS/OMMT nanocomposites containing varied amounts of *p*-MS units in the PE matrix, though still unstable against melting, were ready for an in situ matrix functionalization to improve the stability of the nanocomposite structure.

3.2. *In situ maleated functionalization of the PE-co-p-MS/OMMT nanocomposites*

Maleated functionalization of the PE-*co*-*p*-MS/OMMT nanocomposites was carried out by suspending the as-polymerized powdery samples in benzene under a nitrogen atmosphere. Benzoyl peroxide (BPO) was used as a free radical generator. The reaction was carried out at 75 °C. Three PE-*co*-*p*-MS/OMMT nanocomposite samples bearing varied amounts of *p*-MS units in the polymer matrix (runs 3–5 in Table 1) were selected to conduct the reaction. The OMMT loadings in these samples varied from 1.50 wt% to 2.28 wt%. All these samples had been confirmed with nano-dispersion of OMMT in the as-polymerized powder form, which, however, was found instable against melting. Table 2 summarizes conditions and results of MA modification of the PE-*co*-*p*-MS/OMMT nanocomposites.

In fact, the conditions chosen for the MA modification of the PE-*co*-*p*-MS/OMMT nanocomposites were adopted from Chung et al.'s work on the MA modification of PE-*co*-*p*-MS copolymers prepared by metallocene catalysts, which had been optimized to enhance the selectivity of the free radical grafting reaction on *p*-MS units. Under these conditions, the as-polymerized PE-*co*-*p*-MS/OMMT nanocomposite with a semicrystalline PE-*co*-*p*-MS copolymer matrix, in a fine powder form, was suspended in a solution, containing solvent, initiator and MA. Like the PE-*co*-*p*-MS net copolymer, the PE-*co*-*p*-MS matrix in the nanocomposite had the *p*-MS side groups only located in the amorphous phase. The swollen amorphous domains provided the physical contacts between *p*-MS groups, initiator, and MA reagent. On the other hand, the secondary CH_2 (backbone) or tertiary CH (backbone) units in the crystalline domains were largely intact.

Fig. 5 plots FTIR spectra of the MA-modified PE-*co*-*p*-MS/OMMT nanocomposite samples. The emergence in all three spectra of the absorbances at 1860 and 1780 cm^{-1}, corresponding to the symmetric and asymmetric stretchings of the two carbonyl groups in succinic anhydride, is a clear evidence of the successful MA modification of the PE-*co*-*p*-MS matrixes. The MA contents were determined using a method described by Chung et al. [28]. The results are included in

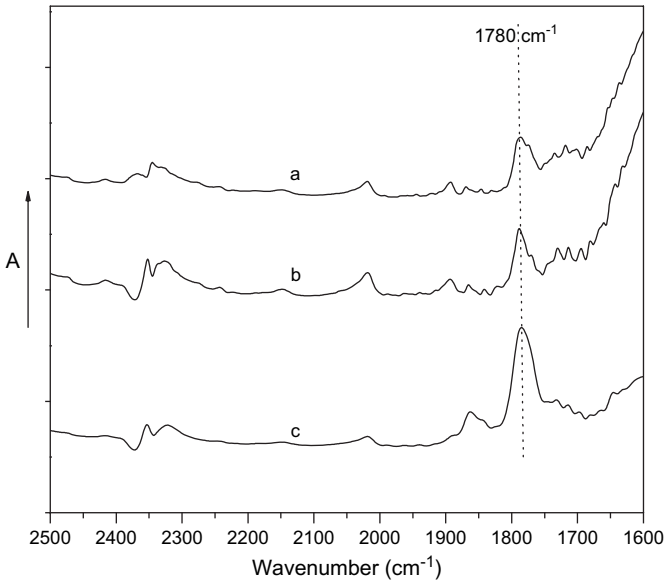

Fig. 5. FTIR spectra of three (PE-*co*-*p*-MS)-*g*-MA/OMMT samples containing (a) 0.27 wt%, (b) 0.30 wt%, and (c) 0.55 wt% of MA groups (runs 1, 2, and 3 in Table 2), respectively.

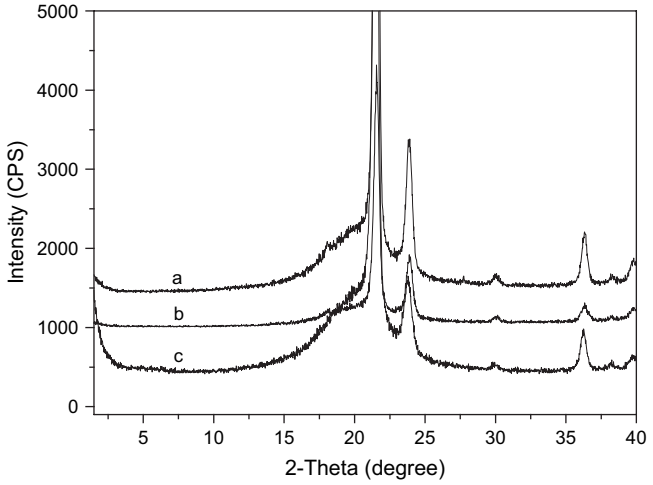

Fig. 6. XRD patterns of three compression-molded (PE-*co*-*p*-MS)-*g*-MA/OMMT samples containing (a) 0.27 wt%, (b) 0.30 wt%, and (c) 0.55 wt% of MA groups (runs 1, 2, and 3 in Table 2), respectively.

Table 2. It is of great interest to note that the graft contents of MA are proportional to the *p*-MS contents of the polymer matrixes, an indication of the selective grafting of MA on the *p*-MS unit. The selective occurrence of the graft reaction was further confirmed by monitoring the alteration of polymer molecular weight before and after modification reaction. The PE-*co*-*p*-MS/OMMT nanocomposite samples, both MA-modified ((PE-*co*-*p*-MS)-*g*-MA/OMMT) and unmodified, were subjected to xylene extraction to retrieve some MMT-free net polymers for viscometry to determine their viscosity-average molecular weights (M_η). A side-by-side comparison of M_η before and after MA modification reveals overall a negligible molecular weight change by the modification reaction except for one sample (run 3 in Table 1 and run 1 in Table 2), which has a *p*-MS content of polymer matrix as low as 0.10 mol%, showing a somewhat noticeable reduction of M_η from 9.72×10^4 to 8.22×10^4 g/mol.

Each MA-functionalized (PE-*co*-*p*-MS)-*g*-MA/OMMT nanocomposite sample was collected in the 15.0 mm × 15.0 mm × 1.0 mm stainless steel chamber and melted at 200 °C for 5 min in between the two hot plates of the compression-molding instrument under a pressure of 8.0 kg cm^{-3}. The specimens were subjected to XRD examination to detect the (001) diffraction peaks of any recovered parallel stacks of MMT that might be induced by polymer melting. Fig. 6 shows XRD patterns of the three samples. It is really fascinating to observe that no sample displays any discernible (001) peak, although they only differ from the unmodified PE-*co*-*p*-MS/OMMT nanocomposites by some small amounts of MA groups in the matrix. This result suggests that the in situ-introduced MA groups in the PE matrix effectively promoted miscibility between the silicate layers of MMT and PE, enhancing the stability of the polymerization-formed nanocomposite structure.

3.3. Functionalization of PE-co-p-MS/OMMT nanocomposite with PMMA side chain

Besides grafting MA group, the benzylic protons (ϕ-CH_3) of *p*-MS unit are also able to undergo effective metallation reaction using butyllithium to generate anionic species in the PE-*co*-*p*-MS matrix that initiates MMA polymerization. A PE-*co*-*p*-MS/OMMT nanocomposite sample (run 5 in Table 1) containing 0.90 mol% of *p*-MS units in the matrix was applied in the anionic PMMA graft reaction. The lithiation reaction was carried out by suspending the as-polymerized powdery nanocomposite sample in THF at 45 °C, using *n*-BuLi and TMEDA as the lithiation reagents. The obtained PMMA-grafted nanocomposite was subjected to boiling acetone extraction for 24 h to remove any PMMA homopolymer (usually less than 10 wt%). The results are included in Table 2.

The obtained (PE-*co*-*p*-MS)-*g*-PMMA/OMMT sample (run 4 in Table 2) contains 10.0 mol% of grafted MMA units, calculated from its ^{1}H NMR spectrum (Fig. 7) using the chemical shift at 3.75 ppm ($-CH_2-(CH_3)C(COOC\mathbf{H}_3)-$). The PMMA-grafted sample was melted at 200 °C for 5 min using the compression-molding instrument. Thus prepared specimen was subjected to XRD examination. Fig. 8 shows the XRD pattern. No (001) peaks due to recovered parallel stacks of MMT are

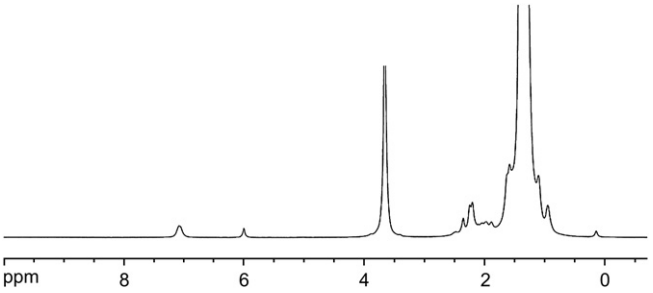

Fig. 7. ^{1}H NMR spectrum of a (PE-*co*-*p*-MS)-*g*-PMMA/OMMT nanocomposite containing 10.0 mol% of MMA units in the matrix (run 4 in Table 2).

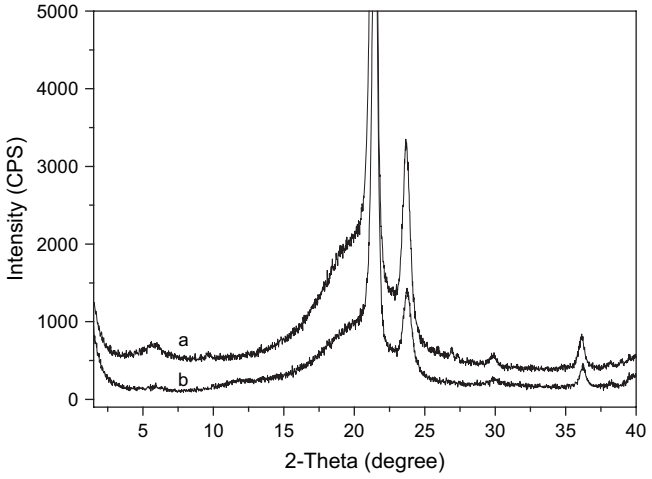

Fig. 8. Comparison of XRD patterns of compression-molded samples of a PE-*co*-*p*-MS/OMMT nanocomposite containing 0.90 mol% of *p*-MS units and 1.50 wt% of OMMT (run 5 in Table 1) (a) before and (b) after grafting PMMA.

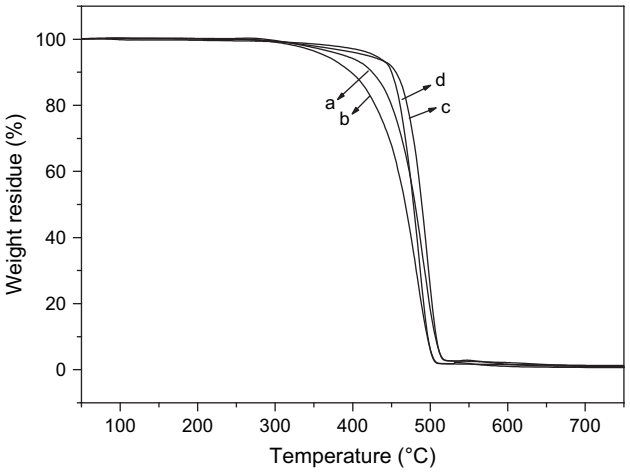

Fig. 9. TGA curves of (a) the as-polymerized, (b) compression-molded, (c) MA- and (d) PMMA-functionalized PE-*co*-*p*-MS/OMMT nanocomposites containing 0.90 mol% of *p*-MS units and 1.50 wt% of OMMT.

discernible. This result suggests that the in situ-introduced PMMA side chains in the PE matrix also promoted miscibility between the silicate layers of MMT and PE matrix, enhancing the stability of the polymerization-formed nanocomposite structure.

3.4. Thermal stability study using TGA

The formation of nanocomposite with MMT usually greatly improves a polymer's thermal stability, due to the laminated silicate layers of MMT functioning as myriad of physical barriers and effectively deterring the thermal transmission in the polymer matrix. In this sense, it is of ease to understand that a collapse (even partially) of the nanocomposite structure leading to silicate layers' re-aggregation will reduce such an effect. The thermal stabilities of the as-polymerized and compression-molded PE-*co*-*p*-MS/OMMT nanocomposites (runs 3, 4, and 5 in Table 1) were studied in air using TGA. The onset decomposition temperatures (T_{onset}) are collected in Table 3. It is found that the T_{onset} values of the compression-molded samples are generally lower than those of the as-polymerized powdery samples. This is consistent with the XRD results showing the collapse of the polymerization-formed nanocomposite structure after compression molding. However, after matrix functionalization, either with MA groups or PMMA side chains, the compression-molded samples (T_{onset} values also listed in Table 3) exhibit much improved thermal stabilities, with the T_{onset} values even higher than those of the as-polymerized ones. Fig. 9 plots the TGA curves of a PE-*co*-*p*-MS/OMMT nanocomposite containing 0.90 mol% of *p*-MS units and 1.50 wt% of OMMT (run 5 in Table 1) in both the as-polymerized and compression-molded forms, and its MA-functionalized and PMMA-grafted counterparts. The in situ-introduced functional groups, including the MA groups and PMMA side chains, through promoting the stability of the polymerization-formed nanocomposite structure, must have effectively enhanced the nano-filling effect of MMT on many of the polymer properties, which certainly include the thermal stability.

Table 3
T_{onset} values from TGA curves of PE-*co*-*p*-MS/OMMT nanocomposites and their corresponding functionalized derivatives

PE-*co*-*p*-MS/OMMT nanocomposite	T_{onset} (°C)			
	Powdery sample	Molded sample	MA-grafted	PMMA-grafted
Entry 3 in Table 1	465.9	457.4	477.5	–
Entry 4 in Table 1	460.7	457.2	463.2	–
Entry 5 in Table 1	459.7	436.3	470.1	469.3

3.5. TEM visualization of nanocomposite structure

Finally, a compression-molded (PE-*co*-*p*-MS)-*g*-MA/OMMT nanocomposite sample (run 1 in Table 2, containing

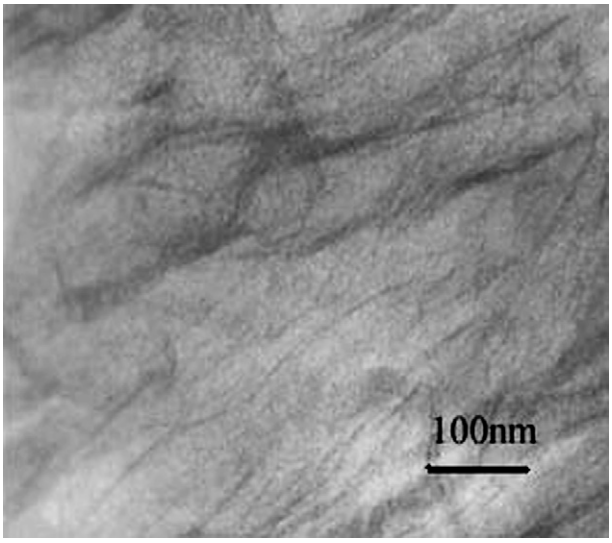

Fig. 10. TEM image of a compression-molded (PE-*co*-*p*-MS)-*g*-MA/OMMT nanocomposite sample (run 1 in Table 2, containing 2.28 wt% of OMMT).

2.28 wt% of OMMT) was subjected to TEM characterization to visualize the stable nanocomposite structure (the exfoliated MMT dispersion in PE matrix). The nanometer-scale silicate layers (ca. 5–15 nm in thickness) were clearly discerned, as illustrated in Fig. 10.

4. Conclusions

In summary, we have demonstrated in this research an effective way for enhancing the structure stability of polyolefin/MMT nanocomposites prepared by intercalative polymerization. By engaging a reactive comonomer, e.g. *p*-MS, in the intercalative polymerization of ethylene using an OMMT (organically modified MMT)-intercalated metallocene catalyst ($Et[Ind]_2ZrCl_2$ in combination with MAO), PE-*co*-*p*-MS/OMMT nanocomposites based on a reactive PE matrix bearing *p*-MS units were obtained. The benzylic protons (ϕ-CH_3) of the incorporated *p*-MS unit in the PE-*co*-*p*-MS matrix were able to undergo, under mild reaction conditions, both free radical maleation reaction and butyllithium-induced metallation reaction, with the latter being followed by an anionic graft-from polymerization of MMA. The in situ-incorporated functional groups, including the pendant maleic anhydride groups and the polar PMMA side chains, effectively improved the miscibility between the PE matrix and laminated silicate layers of MMT, leading to significant enhancement of the stability of the nanocomposite structure against processing.

A further detailed research is being focused on both the qualitative and quantitative correlations between the types, concentrations, and distributions of functional groups and the extents to which the structure stability will be enhanced. Those results will be reported elsewhere.

Acknowledgements

Financial supports from the National Science Foundation of China (Grant nos. 20304017, 50373048, 50573081 and 20334030) and Ministry of Science and Technology of China (“973” project, G2003 CB615600) are gratefully acknowledged.

References

[1] Kawasumi M. J Polym Sci Part A Polym Chem 2004;42:819.
[2] Ray SS, Okamoto M. Prog Polym Sci 2003;28:1529.
[3] Usuki A, Hasegawa N, Kato M. Adv Polym Sci 2005;179:135.
[4] Galli P, Vecellio G. J Polym Sci Part A Polym Chem 2004;42:396.
[5] Manias E, Touny A, Wu L, Strawhecker K, Lu B, Chung TC. Chem Mater 2001;13:3516.
[6] Tudor J, Willington L, O’Hare D, Royan B. Chem Commun 1996; 2031.
[7] Bergman JS, Chen H, Giannelis EP, Thomas MG, Coates GW. Chem Commun 1999;2179.
[8] Sun T, Garce’s JM. Adv Mater 2004;14:128.
[9] Heinemann J, Reichert P, Thomann R, Mulhaupt R. Macromol Rapid Commun 1999;20:423.
[10] Alexandre M, Dubois P, Sun T, Garces JM, Jerome R. Polymer 2002;43:2123.
[11] Lee DH, Kim HS, Yoon KB, Min KE, Seo KH, Noh SK. Sci Technol Adv Mater 2005;6:457.
[12] Ray S, Galgali G, Lee A, Sivaram S. J Polym Sci Part A Polym Chem 2005;43:304.
[13] Dubois P, Alexandre M, Jerome R. Macromol Symp 2003;194:13.
[14] Liu C, Tang T, Wang D, Huang B. J Polym Sci Part A Polym Chem 2003;41:2187.
[15] Vaia RA, Giannelis EP. Macromolecules 1997;30:7990.
[16] Balazs AC, Singh C, Zhulina E, Lyatskaya Y. Acc Chem Res 1999;32(8):651.
[17] Jin YH, Park HJ, Im SS, Kwak SY, Kwak SJ. Macromol Rapid Commun 2002;23:135.
[18] He AH, Hu HQ, Huang YJ, Dong JY, Han CC. Macromol Rapid Commun 2004;25:2008.
[19] Huang YJ, Yang KF, Dong JY. Macromol Rapid Commun 2006; 27:1278.
[20] Zhang XF, Chen ST, Li HY, Zhang ZC, Lu YY, Wu CH, et al. J Polym Sci Part A Polym Chem 2007;45:59.
[21] Hakala K, Helaja T, Löfgren B. J Polym Sci Part A Polym Chem 2000;38:1966.
[22] Paavola S, Löfgren B, Seppälä JV. Eur Polym J 2005;41:2861.
[23] Kawahara N, Kojoh S, Matsuo S, Kaneko H, Matsugi T, Kashiwa N. J Mol Catal A Chem 2005;241:156.
[24] Chung TC, Lu HL. J Polym Sci Part A Polym Chem 1997;35:575.
[25] Chung TC, Lu HL, Ding RD. Macromolecules 1997;30:1272.
[26] Chung TC, Lu HL. J Polym Sci Part A Polym Chem 1998;36:1017.
[27] Lu HL, Chung TC. J Polym Sci A Polym Chem 1999;37:4176.
[28] Lu B, Chung TC. J Polym Sci A Polym Chem 2000;38:1337.
[29] Sano T, Doi K, Hagimoto H, Wang Z, Uozumi T, Soga K. Chem Commun 1999;733.
[30] Oaman MA, Rupp JEP, Suter UW. Polymer 2005;46:1653.